ACS APPLIED MATERIALS & INTERFACES

Research Article

www.acsami.org

High-Resolution Colorimetric Assay for Rapid Visual Readout of Phosphatase Activity Based on Gold/Silver Core/Shell Nanorod

Zhuangqiang Gao,[†] Kaichao Deng,[†] Xu-Dong Wang,[‡] Manuel Miró,[§] and Dianping Tang*,[†]

[†]Institute of Nanomedicine and Nanobiosensing, MOE Key Laboratory of Analysis and Detection for Food Safety, Department of Chemistry, Fuzhou University, Fuzhou 350108, China

[‡]Karlsruhe Institute of Technology (KIT), Institute for Biological Interfaces (IBG-1), Hermann-von-Helmholtz-Platz 1, D-76344 Eggenstein-Leopoldshafen, Germany

[§]FI-TRACE Group, Department of Chemistry, Faculty of Science, University of the Balearic Islands, 07122 Palma de Mallorca, Illes Balears, Spain

Supporting Information

ABSTRACT: Nanostructure-based visual assay has been developed for determination of enzymatic activity, but most involve in poor visible color resolution and are not suitable for routine utilization. Herein, we designed a high-resolution colorimetric protocol based on gold/silver core/shell nanorod for visual readout of alkaline phosphatase (ALP) activity by using bare-eyes. The method relied on enzymatic reaction-assisted silver deposition on gold nanorod to generate significant color change, which was strongly dependent on ALP activity. Upon target ALP introduction into the substrate, the ascorbic acid 2-phosphate was hydrolyzed to form ascorbic acid, and then, the generated ascorbic acid reduced silver ion to metal silver and coated on the gold nanorod, thereby resulting in the blue shift of longitudinal localized surface plasmon resonance peak of gold nanorod accompanying a perceptible color change from red to orange to yellow to green to cyan to blue and to violet. Under optimal conditions, the designed method exhibited the wide linear range 5−100 mU mL^{-1} ALP with a detection limit of 3.3 mU mL^{-1}. Moreover, it could be used for the semiquantitative detection of ALP from 20 to 500 mU mL^{-1} by using the bare-eyes. The coefficients of variation for intra- and interassay were below 3.5% and 6.2%, respectively. Finally, this method was validated for the analysis of real-life serum samples, giving results matched well with those from the 4-nitrophenyl phosphate disodium salt hexahydrate (pNPP)-based standard method. In addition, the system could even be utilized in the enzyme-linked immunosorbent assay (ELISA) to detect IgG at picomol concentration. With the merits of simplification, low cost, user-friendliness, and sensitive readout, the gold nanorod-based colorimetric assay has the potential to be utilized by the public and opens a new horizon for bioassays.

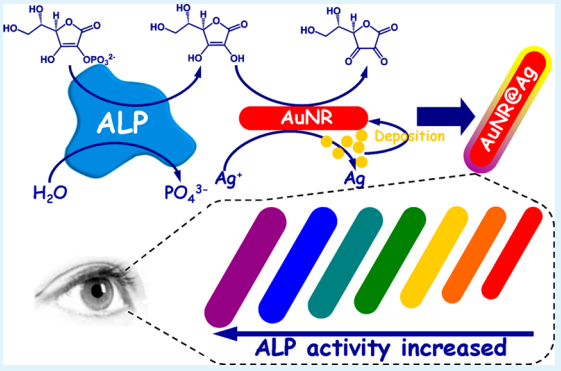

KEYWORDS: *alkaline phosphatase, gold nanorod, localized surface plasmon resonance, high-resolution colorimetric assay, bare-eyes*

1. INTRODUCTION

Enzymatic reactions play major roles in nearly every living organism. Even in a single cell, there exist thousands of enzymatic reactions to provide resources and energy for normal metabolism and proliferation.[1,2] All the enzymatic reactions are precisely controlled similar to a well-programmed machine. The dysfunction of each enzymatic reaction may induce severe diseases and even may threaten a cell's life. One of the major causes of the dysfunction is the changing of enzyme activity.[1,3] Therefore, the measurement and monitoring of enzymatic activity in biological fluids has become increasingly important. Up to now, many approaches have been developed for this purpose based on various techniques including fluorescence, chemiluminescence, Raman, and electrochemistry.[4−7] Despite their high sensitivity and selectivity, these assays have some limitations including the use of sophisticated instruments with complicated data-collecting/or -processing systems, and a relatively long analysis time, thereby limiting their wide acceptance.[8,9] For example, fluorescence resonance energy transfer is widely employed for enzymatic activity assays. However, it often involves the pair of fluorescence label and quencher.[4] In contrast, colorimetric assays display obvious advantages due to their simplicity, convenience, practicality, low cost, and rapid/direct readout using bare-eyes.[10−12] Generally, conventional colorimetric assays are based upon the specific reaction between certain enzyme and the corresponding substrate or chromogenic agents to generate color change.[13−15] Unfortunately, most of them suffer from low color resolution

Received: August 9, 2014
Accepted: September 22, 2014
Published: September 22, 2014

 © 2014 American Chemical Society

Scheme 1. Schematic Illustration of the High-Resolution Colorimetric Assay for Sensitive Visual Readout of Phosphatase Activity Based on Gold/Silver Core/Shell Nanorod

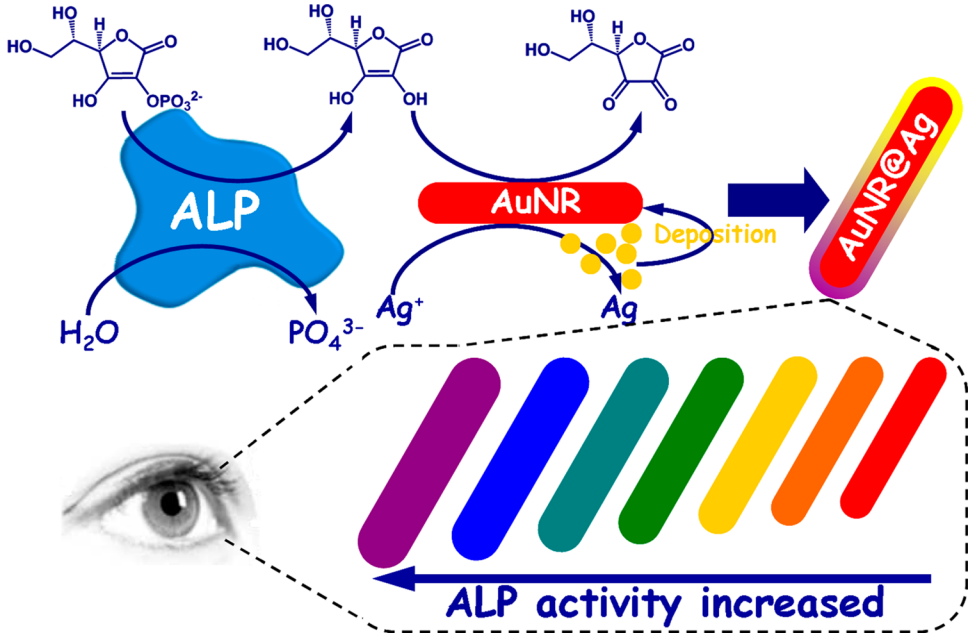

and thus only serve as a rough estimation. Hence, the exploration of novel colorimetric assay protocols for visual monitoring of enzyme activities with high color resolution and high sensitivity is of great significance.

Plasmonic noble metal (e.g., gold and silver) nanostructures attract substantial research interest yesteryears due to their rich, intriguing, and complex optical properties originating from the excitation of surface plasmon resonances.[16−20] Among these metallic nanostructures, gold nanorod (AuNR) holds great potential as the next-generation of plasmonic transducer in assays and sensor systems because of its elongated nanostructure, sharp/polarized near-infrared resonance, and tunable plasmon resonant spectra.[21−24] In particular, its localized surface plasmon resonance (LSPR) absorption is extremely sensitive to the size, composition, distance, and the surrounding media, based on which great progress in colorimetric sensors have been made.[21,25] Recent experiments have demonstrated that the LSPR absorption of AuNR could be precisely tuned by depositing silver nanoshell on their surface, which can lead to apparent multicolor change.[26,27] This phenomenon has been successfully proved to be highly useful in chemical sensing systems for monitoring time, temperature, and food freshness.[27] However, the application of the intriguing phenomenon for the detection of biomolecules in real-life biological samples is still scarce.

Herein, we explore the fascinating phenomenon to design a simple but effective strategy for direct readout of phosphatase activity by using bare-eyes with high color resolution, accompanying with a rainbow-like multicolor change (Scheme 1). We employ alkaline phosphatase (ALP) as a model enzyme because it is often used as an indicator of hepatobiliary and bone disorder, breast and prostatic cancer, and diabetes in clinical diagnostics.[28] Moreover, it is also one of the most commonly used enzyme labels in the bioanalysis.[29] In this work, the ALP hydrolyzes ascorbic acid 2-phosphate (AA-P) into ascorbic acid (AA). Then, the produced AA (as a common reduction reagent in chemical reactions[30]) reduces silver ion to generate a silver nanoshell on the surface of AuNR. This leads to the blue shift of longitudinal LSPR peak of AuNR, accompanying with a perceptible color change from red to orange to yellow to green to cyan to blue and to violet. The change of the color and the longitudinal LSPR peak depends on the amount of the produced silver nanostructure deposited on the AuNR, thus indirectly relying on the ALP activity. By monitoring the change in the color/or the longitudinal LSPR peak, we can (semi-) quantitatively determine the activity of target ALP in real-life biological samples.

2. EXPERIMENTAL SECTION

Material and Reagent. Cetyltrimethylammonium bromide (CTAB) and Tween 20 were purchased from Genview (U.S.A.). Chloroauric acid tetrahydrate ($HAuCl_4{\cdot}4H_2O$), silver nitrate ($AgNO_3$) and bovine serum albumin (BSA) were acquired from Sinopharm Chem. Re. Co., Ltd. (Shanghai, China). Diethanolamine (DEA, Aladdin, China), L-ascorbic acid (AA, Fluka, U.S.A.), alkaline phosphatase (ALP, Toyobo, Japan), 4-nitrophenyl phosphate disodium salt hexahydrate (pNPP, Alfa Aesar, China), and L-ascorbic acid 2-phosphate sesquimagnesium salt hydrate (AA-P, Sigma-Aldrich, U.S.A.) was used throughout the work. Goat polyclonal antirabbit IgG antibody (Ab_1, Jackson ImmunoResearch Laboratories Inc., U.S.A.), ALP-labeled goat polyclonal antirabbit IgG antibody (ALP-Ab_2, Vector Laboratories Inc., U.S.A.), and Rabbit IgG (RIgG, Dingguo Biotechnol. Inc., China) were utilized for the development of colorimetric immunoassay. All high-binding polystyrene 96-well single-break strip plates were purchased from Greiner Bio-One (Frickenhausen, 705071, Germany). All other reagents were of analytical grade without further purification. Millipore purification system-based ultrapure water was used in this study (18.2 MΩ cm^{-2}, Milli-Q, Millipore). Human serum specimens derived from Fujian Provincial Hospital, China.

Three types of DEA buffer solutions including 0.1 mol L^{-1} of pH 7.6 DEA buffer [1.0514 g DEA + 0.0257 g $Mg(NO_3)_2{\cdot}6H_2O$], 0.4 mol L^{-1} of pH 9.8 DEA buffer [4.207 g DEA + 0.0513 g $Mg(NO_3)_2{\cdot}6H_2O$], and 1.0 mol L^{-1} of pH 9.8 DEA buffer [10.514 g DEA + 0.0257 g $Mg(NO_3)_2{\cdot}6H_2O$] were prepared by adding the corresponding chemicals in 100 mL distilled water, respectively, and adjusted to the desired pH by using HNO_3. A pH 9.6 carbonate buffer [1.69 g Na_2CO_3 + 2.86 g $NaHCO_3$] and a 0.01 mol L^{-1} of pH 7.4 phosphate-

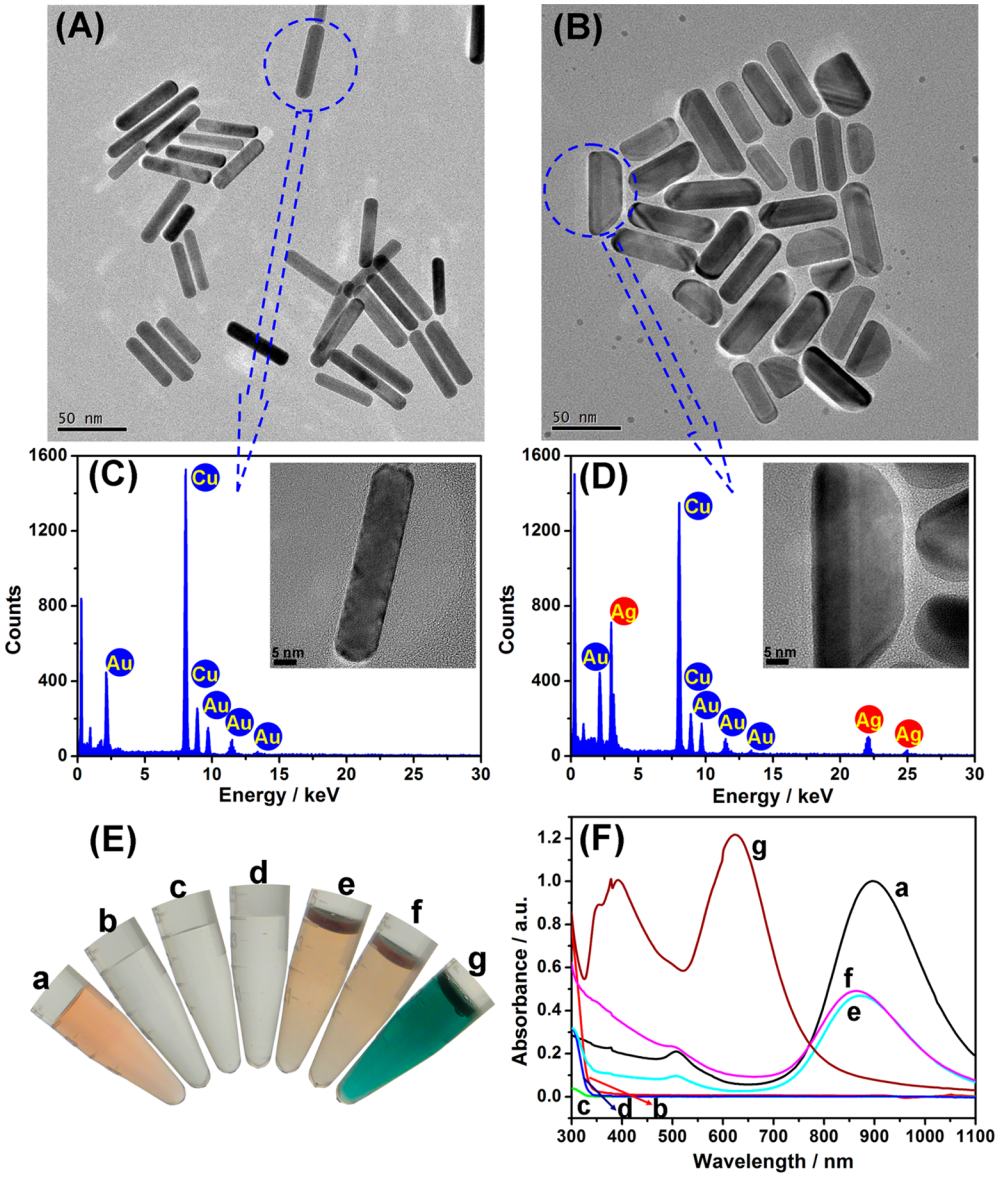

Figure 1. (A, B) TEM images of AuNR before (A) and after (B) silver deposition. (C, D) EDX spectra of corresponding areas of A, B, respectively (Inserts: the corresponding high-resolution TEM images). (E) Photographs and (F) UV−vis absorption spectra of (a) AuNR, (b) AA-P in 0.4 mol L^{-1} DEA buffer (pH 9.8), (c) $AgNO_3$, (d) ALP, (e) AuNR + buffer, (f) AuNR + AA-P + $AgNO_3$ + buffer, and (g) AuNR + AA-P + $AgNO_3$ + ALP + buffer.

buffered saline [PBS, 2.9 g $Na_2HPO_4 \cdot 12H_2O$ + 0.24 g KH_2PO_4 + 0.2 g KCl + 8.0 g NaCl] solution were prepared by adding the corresponding chemicals in 1000 mL distilled water, respectively. The washing and blocking solutions were acquired by adding 0.05% Tween 20 (v/v) and 1.0% (w/v) BSA in PBS, respectively.

Synthesis of Gold Nanorod (AuNR). Gold nanorod (designated as AuNR) was synthesized by using a classical seed-mediated growth method.[31−33] Initially, two solutions were prepared as follows: a seed solution including 0.6 mL of 0.01 mol L^{-1} $NaBH_4$ (ice-cold), 0.25 mL of 0.01 mol L^{-1} $HAuCl_4$, and 9.75 mL of 0.1 mol L^{-1} CTAB (Note: The solution was quiescently left at room temperature for 2 h before use) and a growth solution containing 40 mL of 0.1 mol L^{-1} CTAB, 2.0 mL of 0.01 mol L^{-1} $HAuCl_4$, 0.4 mL of 0.01 mol L^{-1} $AgNO_3$, 0.8 mL of concentrated HCl, and 0.32 mL of 0.1 mol L^{-1} AA. Afterward, 200 μL of the seed solution was added quickly into the growth solution and stored overnight at room temperature. Following that, the mixture was centrifuged for 20 min at 7000*g*, and the obtained pellet (i.e., AuNR) was suspended into distilled water with an expected optical density of 1.000 ± 0.005 au at 896 nm (Note: During the experiment, the added CTAB mainly acted as a stabilizer, which could prevent the as-synthesized AuNR from aggregation together[18,27]). The as-prepared AuNR was characterized by UV−vis absorption spectroscopy, which exhibited the longitudinal and transverse plasmon bands at 896 and 507 nm, respectively.

Monitoring of ALP Activity Using AuNR-Based Colorimetric Assay Protocol. Before measurement, a substrate solution including 200 μL of 10 mmol L^{-1} AA-P in 0.4 mol L^{-1} DEA buffer (pH 9.8), 20 μL of 10 mmol L^{-1} $AgNO_3$, and 200 μL of AuNR colloids (1.0 au at 896 nm) was initially prepared. Afterward, 10 μL of ALP standards with various activities in the DEA buffer (0.1 mol L^{-1}, pH 7.6) or blank serum sample was added into the substrate solution, and incubated for 60 min at 37 °C. The resulting suspension was monitored, using UV−vis absorption spectroscopy (UV 1102 spectrophotometer, Shanghai Techcomp Co. Ltd., China) within the wavelength range 1100−300 nm.

Monitoring of ALP Activity Using pNPP-Based Assay Protocol. Initially, 10 μL of ALP standards with various activities in 0.1 mol L^{-1} DEA buffer (pH 7.6) or blank serum sample was added

into 400 μL of 1.0 mol L^{-1} DEA buffer (pH 9.8) containing 5.0 mmol L^{-1} pNPP. Then, the resulting mixture was incubated 60 min at 37 °C. After that, UV−vis absorption spectroscope of the mixture was recorded by using UV 1102 spectrophotometer from 550 to 350 nm.

AuNR-Based Colorimetric Immunoassay Protocol for RIgG. Prior to the colorimetric immunoassay, the capture antibody-functionalized microplate was prepared as follows: 50 μL per well of 10 μg mL^{-1} Ab_1 in the carbonate buffer (pH 9.6) was added into the high-binding 96-well single-break strip plate and incubated 12 h at 4 °C. Following that, the Ab_1-modified microplate was washed by using the washing buffer. 300 μL per well of the blocking buffer was injected in the microplate and incubated for 60 min at 37 °C. During this process, the capture antibody (Ab_1) was immobilized on the single-break strip plate. Afterward, the as-prepared microplate was used for the detection of target RIgG. Initially, 50 μL of RIgG standards with different concentrations was added into the well by using pipet and then incubated for 60 min at 37 °C. After that, 50 μL of ALP-Ab_2 was thrown into the well and incubated for another 60 min under the same conditions to form the sandwiched immunocomplex. Subsequently, 100 μL of 10 mmol L^{-1} AA-P in 0.4 mol L^{-1} DEA buffer (pH 9.8), 10 μL of 10 mmol L^{-1} $AgNO_3$, and 100 μL AuNR (1.0 au at 896 nm) were added into the well and reacted for 60 min at 37 °C for the development of visual color. Finally, the produced color solution was diluted by using 200 μL distilled water and measured using UV 1102 spectrophotometer from 1100 to 300 nm (Note: After each step, the microplate was washing with the washing buffer).

3. RESULTS AND DISCUSSION

Characteristics and Control Tests for AuNR-Based Colorimetric Assay. In this work, the detectable colorimetric signal mainly derives from the enzyme-induced silver deposition on the surface of the AuNR. One precondition for the development of AuNR-based colorimetric assay was whether the AuNR could be successfully synthesized via the seed-medicated growth method.[31−33] To demonstrate this point, the morphology of the as-synthesized AuNR was characterized by using transmission electron microscope (TEM, TECNAI G2F20, FEI). As seen from Figure 1A, the as-synthesized nanostructures were well-defined nanorods with a mean length of 55 ± 5 nm and a width of 12 ± 1 nm along the longitudinal axes. Logically, another concern for the AuNR arises to whether the enzyme-catalyzed silver deposition on the AuNR could be smoothly progressed in the presence of ALP, as described in Scheme 1. To clarify this issue, several control tests were implemented under the different conditions by using visual color readout (Figure 1E) and UV−vis absorption spectrophotometer (Figure 1F). The as-prepared AuNR colloids were red (photograph a in Figure 1E) with a longitudinal plasmon peak at 896 nm and a transverse one at 507 nm (curve a in Figure 1F). When 200-μL AuNR (1.0 au at 896 nm) was dispersed in 200-μL of 0.4 mol L^{-1} diethanolamine (DEA) buffer (pH 9.8), the color was almost the same relative to pure AuNR colloids (photograph e). Moreover, the color of AuNR colloids was not changed even if 200-μL AA-P (10 mmol L^{-1}) and 20-μL $AgNO_3$ (10 mmol L^{-1}) were added (photograph f). Further, the longitudinal LSPR peaks of AuNR were not shifted nearly (curve f vs curve e vs curve a). When 10-μL ALP (300 mU mL^{-1}), AA-P, and $AgNO_3$ were introduced into the AuNR colloids, the color of the suspension favorably changed from red to cyan (photograph g), and the longitudinal LSPR peak gradually shifted from 872 to 624 nm (curve g vs curve e) (Note: The absorbance also increased from 0.4691 to 1.2182). The reason might be the fact that the AA obtained by the hydrolysis of AA-P with the aid of ALP could reduce silver ion to form silver nanoshell on the surface of AuNR.

Further, the formation of silver nanoshell on the AuNR was further confirmed by using TEM. As seen from Figure 1B, the reaction of the AuNR with ALP, AA-P, and $AgNO_3$ produced rod-like nanostructures. Apparently, the size of the as-produced nanostructures was significantly larger than that of AuNR (Figure 1B vs A). Previous studies have shown that metal silver more readily deposited on the transverse axis of the AuNR than that at the both ends.[18,27,34] As seen from Figure 1B and Figure 1D, we also observed that the deposited silver on the AuNR in the transverse direction was obviously thicker than that in the longitudinal direction, which resulted in the decrease of the aspect ratio of the nanorod. Moreover, it is well-known that the plasmon resonance wavelength of silver nanocrystals is shorter than that of gold nanocrystals under the same size and shape.[18,27] Both the decrease in the aspect ratio of the nanostructure and the increase in the optical properties of silver nanoshell over those of gold nanocore could cause the blue shift of the longitudinal LSPR peak and enhance the absorbance intensity of the hybrid nanostructure. Meanwhile, we also used the energy-dispersive X-ray (EDX) to characterize the individual nanostructures before and after reaction with ALP, AA-P, and $AgNO_3$. As shown in Figure 1D, the nanoshell on the AuNR originated from the metallic silver as compared to Figure 1C. Moreover, the characteristic absorption peak of silver colloids could be observed at 403 nm, which also indicated the formation of silver nanostructures after the reaction of AuNR with ALP, AA-P, and $AgNO_3$ (curve g in Figure 1F).[35,36] These results confirmed that the blue shift of the longitudinal LSPR peak of AuNR and the color change of the AuNR solution were attributed to ALP-induced silver deposition on the AuNR.

To further demonstrate our design, other control tests including AuNR + AA-P, AuNR + $AgNO_3$, AuNR + ALP, AuNR + ALP + AA-P ,and AuNR + ALP + $AgNO_3$ were also studied, respectively. As indicated from Figure S1 in the Supporting Information, target ALP alone could not cause the change of the longitudinal LSPR peak of AuNR regardless of the presence of AA-P or $AgNO_3$. A puzzling question posed was to discern whether the AA produced by ALP-hydrolyzed AA-P could readily induce the blue shift of the longitudinal LSPR peak of AuNR. As shown in Figure S2 in the Supporting Information, the mixture including AuNR, $AgNO_3$, and AA after incubation for different times could lead to a similar blue shift of the longitudinal LSPR peak of AuNR. These results further corroborated that the production of AA by the biocatalytic activity of ALP toward AA-P was the key factor in this work for the reduction of silver ion to generate silver nanoshell on the surface of AuNR, thus leading to the blue shift of the longitudinal LSPR peak and the color change of the AuNR solution, which is in good agreement with previous reports.[27,37−39]

Optimization of Experimental Conditions for AuNR-Based Colorimetric Assay. Based on ALP manufacturer suggestion (http://www.toyobo-global.com/seihin/xr/lifescience/products), the ALP experiments should be better carried out at an effective working pH of 9.8 and an effective incubation temperature of 37 °C. Under these conditions, other possible experimental parameters including AA-P concentration, $AgNO_3$ concentration, DEA concentration, and the deposition time for metal silver should be investigated in detail. In this work, the progression of the colorimetric assay

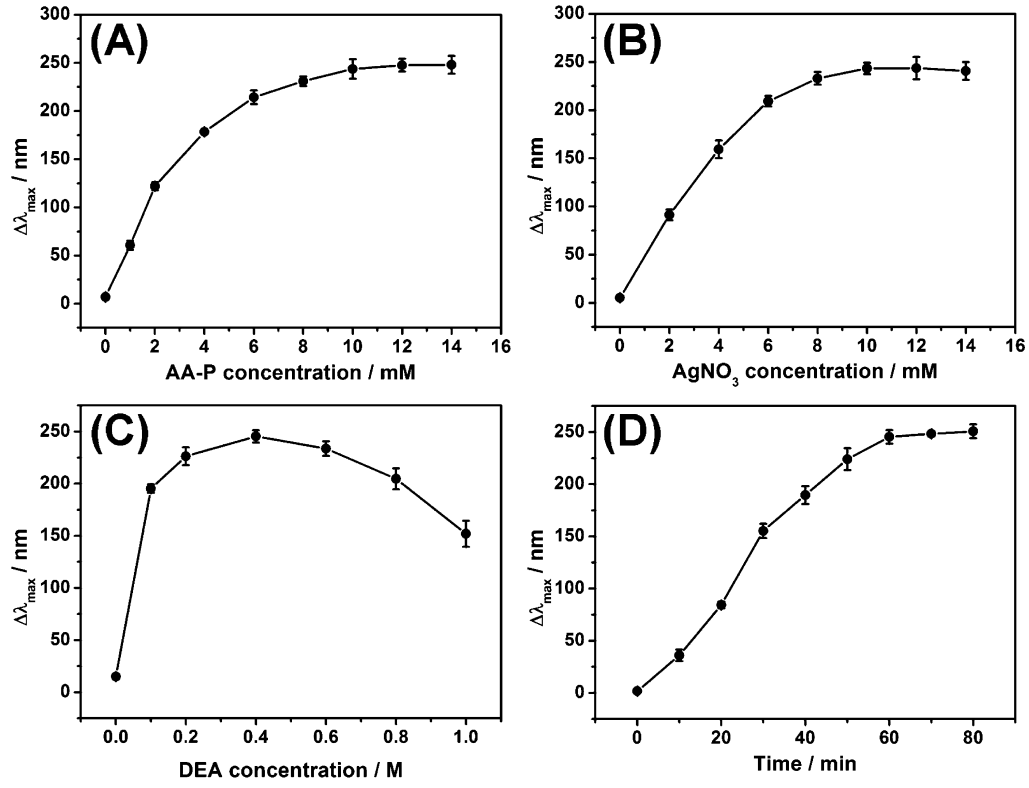

Figure 2. Effects of (A) AA-P concentration, (B) $AgNO_3$ concentration, (C) DEA concentration, and (D) reaction time for silver deposition on the blue shift in the longitudinal LSPR peak of the AuNR. Error bar represents the standard deviation (n = 3).

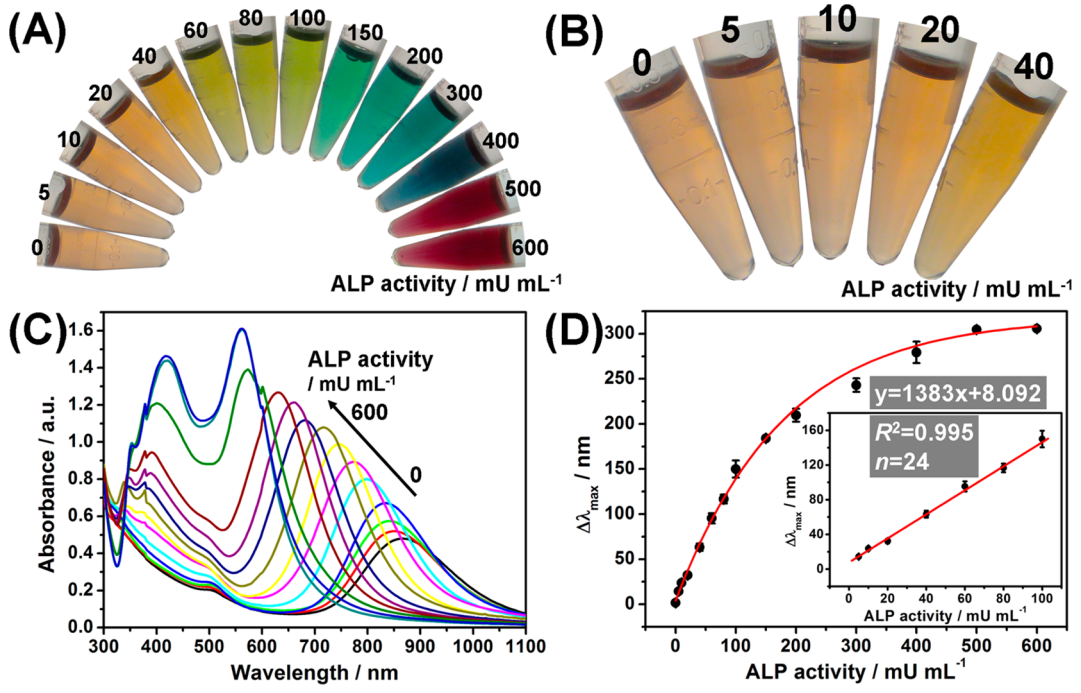

Figure 3. (A) Photographs of the colorimetric assay toward ALP standards with different activities, (B) magnification photographs toward 0, 5, 10, 20, and 40 mU mL^{-1} ALP, (C) UV−vis absorption spectra of the colorimetric assay toward various-activities of ALP, and (D) calibration plots based on LSPR peak shift of maximum wavelength change with ALP activity (Inset: Linear curve). Error bar represents the standard deviation (n = 3).

mainly stemmed from the ALP-catalyzed hydrolysis of AA-P toward the reduction of silver ions. Thus, the concentrations of AA-P and $AgNO_3$ in the detection solution were expected to affect the formation of silver nanoshell. As seen from Figure 2A and B, the signal increased with the increase of AA-P/$AgNO_3$ concentration and tended to level off after 10 mmol L^{-1} AA-P and 10 mmol L^{-1} $AgNO_3$. Therefore, 10 mmol L^{-1} AA-P and 10 mmol L^{-1} $AgNO_3$ were used for the colorimetric assay.

Typically, the DEA used in this study not only offers the alkaline environment for the catalytic hydrolysis of ALP toward

dx.doi.org/10.1021/am505342r | ACS Appl. Mater. Interfaces 2014, 6, 18243−18250

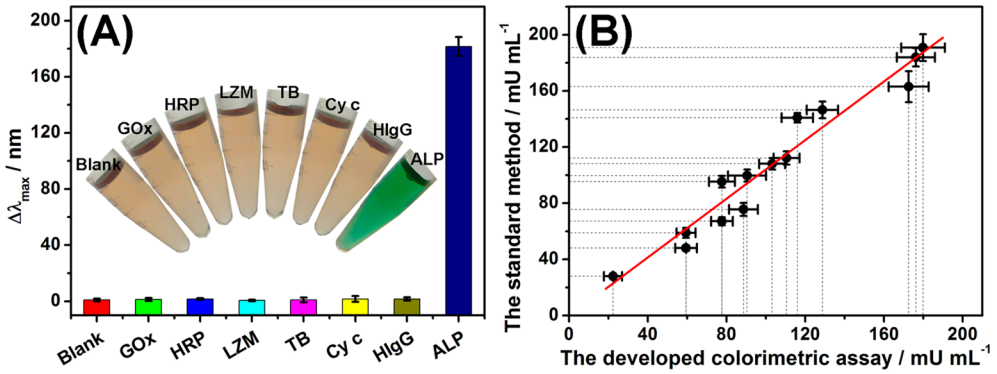

Figure 4. (A) Specificity of the colorimetric assay against ALP (150 mU mL^{-1}), GOx (1.0 μg mL^{-1}), HRP (1.0 μg mL^{-1}), LZM (1 μg mL^{-1}), TB (1.0 μmol L^{-1}), Cyc (5.0 μmol L^{-1}), and HIgG (1.0 μg mL^{-1}) (Inset: The corresponding photographs), and (B) comparison of the assay results toward ALP in real-life clinical serum specimens using the developed colorimetric assay and the pNPP-based standard method, respectively. Error bar represents the standard deviation (n = 3).

AA-P but also is crucial for preventing the formation of the silver hydroxide precipitate under alkaline conditions.[37] As shown in Figure 2C, the blue shift in the longitudinal LSPR peak initially increased with the increment of DEA concentration from 0 to 0.4 mol L^{-1}, and then decreased. The maximum blue shift occurred at 0.4 mol L^{-1} DEA. Thus, 0.4 mol L^{-1} DEA buffer (pH 9.8) was employed as a substrate buffer for the development of the colorimetric assay.

In addition, the deposition time for silver nanoshell on the AuNR directly affects the change of visible color. As indicated from Figure 2D, the blue shift in the longitudinal LSPR peak increased with the increase in the reaction time and almost reached steady-state conditions after 60 min. Longer reaction time did not cause obvious significant increase in the blue shift. Therefore, a reaction time of 60 min was used for the remainder of the study.

Analytical Performance for AuNR-Based Colorimetric Assay. Under optimal conditions, the sensitivity and dynamic measurement range of the colorimetric assay were evaluated against ALP standards by using gold/silver core/shell nanorod as the color indicator. As seen from Figure 3A and B, the solution presented distinct color changes from red to orange to yellow-green to green to cyan to blue and to violet with a high resolution up to 20 mU mL^{-1} toward ALP activity below 500 mU mL^{-1} (Note: The basic theoretical analysis of how silver nanoshell influences the LSPR peak and color of the AuNR is described and discussed in the literature[40,41]). The rainbow-like color change could be easily identified by using bare-eyes or analyzed by using a charge-coupled device camera for quantitative analysis via digital imaging,[42,43] because the resolving power of the bare-eyes toward different color change (ca. 10 million color types) is much more sensitive than that of intensity change in homochromatism (ca. 64 grades).[9] Further, we used UV−vis absorption spectra to quantitatively monitor the change of the colorimetric assay in the absorbance toward ALP with different activities (Figure 3C). The longitudinal LSPR peak gradually shifted from 865 to 560 nm, and the absorbance of the longitudinal LSPR peak increased with the increase of ALP activity. The calibration plots displayed a good linear relationship between the blue shifts of the longitudinal LSPR peak ($\Delta\lambda_{max}$) and ALP activities in the range from 5 mU mL^{-1} to 100 mU mL^{-1} with a detection limit (LOD) of 3.3 mU mL^{-1} ALP based on 3σ_b/slope, where σ_b was the standard deviation of blank samples (Figure 3D). For comparison, we also investigated the analytical properties of the colorimetric assay for quantitative detection of ALP activity in blank human serum (see Figure S3 in the Supporting Information). In this case, the LOD was 14.5 mU mL^{-1} ALP, which was higher than that in buffer. Because the threshold of total ALP in human serum is ∼30 mU mL^{-1},[44] the colorimetric assay could meet the requirement of clinical diagnostics of ALP activity in human serum. Although the nanostructures were made of gold and silver, the assay would still be very inexpensive. All the chemicals used in one sample test were less than two cent—US $0.0152 (based on the reagents' cost, please see the detailed calculation process in the Supporting Information). These results indicated that the developed colorimetric assay was a simple, sensitive, equipment-free, and cost-effective method for ALP activity monitoring.

The repeatability and intermediate precision of the colorimetric assay were evaluated by calculating intra/inter-batch coefficients of variation (CVs, n = 6). Experimental results indicated that the CVs by using the same-batch AuNR and different-batch AuNR were 2.6%, 3.5%, and 1.3% for the intra-assay, and 6.2%, 5.6%, and 3.8% for the interassay toward 40 mU mL^{-1}, 150 mU mL^{-1}, and 500 mU mL^{-1} ALP, respectively. The low CVs indicated that the colorimetric assay could be used for mass production to measure ALP activity.

The selectivity of the colorimetric assay was evaluated using common enzymes or substances as competitors, including glucose oxidase (GOx), horseradish peroxidase (HRP), lysozyme (LZM), thrombin (TB), cytochrome c (Cyc), and human IgG (HIgG). As shown in Figure 4A, a significant change in the blue shift was observed only with target ALP relative to the higher interfering components, which revealed that the assay has a good selectivity toward ALP detection.

Further, we also investigated the stability of the as-synthesized AuNR during a long-time period. When not in use, the as-prepared AuNR was statically placed at room temperature by using CTAB as the stabilizer[18,27] and measured intermittently toward the same-concentration ALP activity. No significant change in the blue shift was acquired after storage for 6 months (Figure S4 in the Supporting Information), indicating that the AuNR could exhibit a long-time stability.

Monitoring of Clinical Human Serum Samples. To further investigate the application possibility of the AuNR-based colorimetric assay for the ALP determination of clinical human serum samples, 14 serum specimens (gifted from the Clinical Laboratory and Medical Diagnostics Laboratory of the local Fujian Provincial Hospital) with different ALP activities

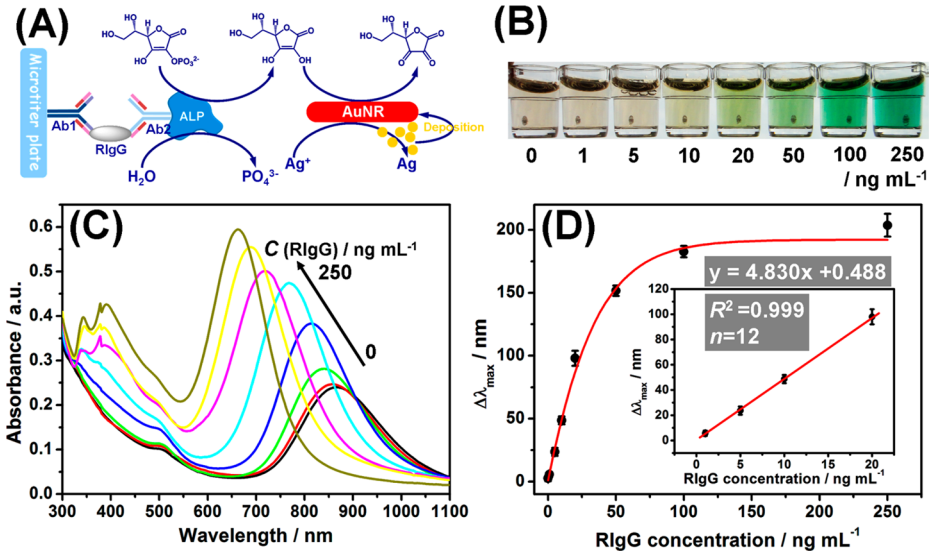

Figure 5. (A) Schematic illustration of the colorimetric assay for enzyme immunoassays, (B) photographs of strategy A toward different-concentration RIgG standards, (C) UV−vis absorption spectra, and (D) calibration plots based on the LSPR peak shift (Inset: Linear curve). Error bar represents the standard deviation (n = 3).

were monitored by using the designed assay protocol. Further, the obtained experimental results on the ALP activity in these serum samples were compared with those from the pNPP-based standard assay method. Figure 4B shows the comparative results with these samples between two methods. As analyzed from these experimental data, a highly positive correlation between the two methods was established, with a slope of 1.05 ± 0.07, an intercept of −1.43 ± 8.16, and a correlation coefficient of 0.973, demonstrating that the results obtained from the developed method correlated well with those from the standard ALP assay within the experimental error. These results strongly confirmed that the AuNR-based colorimetric assay was reliable for real-life serum samples detection.

Application of AuNR-Based Colorimetric Assay in the Sandwiched Immunoassay. We further explored and extended the colorimetric assay into other biological analyses by using the ALP as the enzyme linker, for example, enzyme-linked immunosorbent assay (ELISA). As shown in Figure 5A, rabbit immunoglobulin G (RIgG) was used as a model analyte and ALP-labeled anti-RIgG antibody was employed as a detection antibody. As seen from Figure 5B, the visible color of the detection solution also turned from red to orange to yellow to yellow-green and to green with the increase of RIgG concentration. Moreover, the method displayed a high sensitivity with an LOD of 1.5 ng mL^{-1} (10 pM) RIgG (Figure 5C and D).

4. CONCLUSIONS

In summary, we demonstrated a high-resolution colorimetric assay for simple and sensitive monitoring of ALP activity via enzyme-assisted silver deposition on the AuNR. Compared with the conventional colorimetric assays, this system is inexpensive (~USD $0.0152 for a single test), rapid (relative to commercialized available ELISA, >3 h), portable, and user-friendly without the need of instrumentation. The methodology demonstrated in this work provided a quick and fast assay for researchers and end-users to monitor enzyme activities by judging different colors by bare-eyes detection. This concept can be further explored for quantitative detection of proteins and development of cost-effective detection kits. In view of the simplification, sensitivity, low cost, user-friendliness, and visual readout with bare-eyes, the colorimetric method reported here has the potential to be used by the public for semiquantitative detection.

■ ASSOCIATED CONTENT

Supporting Information

Additional information as noted in text including the control tests (Figure S1 and Figure S2), analysis of human serum samples (Figure S3), and the stability of the AuNR (Figure S4). This material is available free of charge via the Internet at http://pubs.acs.org.

■ AUTHOR INFORMATION

Corresponding Author

*Phone: +86-591-2286-6125. Fax: +86-591-2286-6135. Email: dianping.tang@fzu.edu.cn.

Notes

The authors declare no competing financial interest.

■ ACKNOWLEDGMENTS

Support by the National Natural Science Foundation of China (Grant Nos. 41176079 and 21475025), the National Science Foundation of Fujian Province (grant no. 2014J0105), and the Program for Changjiang Scholars and Innovative Research Team in University (Grant No. IRT1116) is gratefully acknowledged.

■ REFERENCES

(1) Lehninger, A. L.; Nelson, D. L.; Cox, M. M. *Lehninger Principles of Biochemistry*, 5th ed; W. H. Freeman: New York, 2008.

(2) Hunter, T. Protein Kinases and Phosphatases: The Yin and Yang of Protein Phosphorylation and Signaling. *Cell* **1995**, *80*, 225−236.

(3) Erickson, J. R.; Pereira, L.; Wang, L.; Han, G.; Ferguson, A.; Dao, K.; Copeland, R. J.; Despa, F.; Hart, G. W.; Ripplinger, C. M.; Bers, D. M. Diabetic Hyperglycaemia Activates CaMKII and Arrhythmias by O-Linked Glycosylation. *Nature* **2013**, *502*, 372−376.

(4) Jang, H.; Lee, J.; Min, D. Graphene Oxide for Fluorescence-Mediated Enzymatic Activity Assays. *J. Mater. Chem. B* **2014**, *2*, 2452−2460.
(5) Wang, X.; Wolfbeis, O. S. Fiber-Optic Chemical Sensors and Biosensors (2008−2012). *Anal. Chem.* **2013**, *85*, 487−508.
(6) Suginta, W.; Khunkaewla, P.; Schulte, A. Electrochemical Biosensor Applications of Polysaccharides Chitin and Chitosan. *Chem. Rev.* **2013**, *113*, 5458−5479.
(7) Wei, H.; Wang, E. Nanomaterials with Enzyme-Like Characteristics (Nanozymes): Next-Generation Artificial Enzymes. *Chem. Soc. Rev.* **2013**, *42*, 6060−6093.
(8) Yan, L.; Zhu, Z.; Zou, Y.; Huang, Y.; Lin, D.; Jia, S.; Xu, D.; Wu, M.; Zou, Y.; Zhou, S.; Yang, C. Target-Responsive "Sweet" Hydrogel with Glucometer Readout for Portable and Quantitative Detection of Non-Glucose Targets. *J. Am. Chem. Soc.* **2013**, *135*, 3748−3751.
(9) Wang, X.; Chen, X.; Xie, Z.; Wang, X. Reversible Optical Sensor Strip for Oxygen. *Angew. Chem., Int. Ed.* **2008**, *47*, 7450−7453.
(10) Song, Y.; Wei, W.; Qu, X. Colorimetric Biosensing Using Smart Materials. *Adv. Mater.* **2011**, *23*, 4215−4236.
(11) Gubala, V.; Harris, L. F.; Ricco, A. J.; Tan, M. X.; Williams, D. E. Point of Care Diagnostics: Status and Future. *Anal. Chem.* **2012**, *84*, 487−515.
(12) Wang, X.; Chen, H.; Zhou, T.; Lin, Z.; Zeng, J.; Xie, Z.; Chen, X.; Wong, K.; Chen, G.; Wang, X. Optical Colorimetric Sensor Strip for Direct Readout Glucose Measurement. *Biosens. Bioelectron.* **2009**, *24*, 3702−3705.
(13) Pavlov, V.; Xiao, Y.; Willner, I. Inhibition of the Acetycholine Esterase-Stimulated Growth of Au Nanoparticles: Nanotechnology-Based Sensing of Nerve Gases. *Nano Lett.* **2005**, *5*, 649−653.
(14) Wei, H.; Chen, C.; Han, B.; Wang, E. Enzyme Colorimetric Assay Using Unmodified Silver Nanoparticles. *Anal. Chem.* **2008**, *80*, 7051−7055.
(15) Ornatska, M.; Sharpe, E.; Andreescu, D.; Andreescu, S. Paper Bioassay Based on Ceria Nanoparticles as Colorimetric Probes. *Anal. Chem.* **2011**, *83*, 4273−4280.
(16) Howes, P. D.; Rana, S.; Stevens, M. M. Plasmonic Nanomaterials for Biodiagnostics. *Chem. Soc. Rev.* **2014**, *43*, 3835−3853.
(17) Yu, K.; Sader, J. E.; Zijlstra, P.; Hong, M.; Xu, Q.; Orrit, M. Probing Silver Deposition on Single Gold Nanorods by Their Acoustic Vibrations. *Nano Lett.* **2014**, *14*, 915−922.
(18) Jiang, R.; Chen, H.; Shao, L.; Li, Q.; Wang, J. Unraveling the Evolution and Nature of the Plasmons in (Au Core)−(Ag Shell) Nanorods. *Adv. Mater.* **2012**, *24*, OP200−OP207.
(19) Wan, X.; Zheng, L.; Gao, F.; Yang, X.; Li, C.; Li, Y.; Huang, C. Real-Time Light Scattering Tracking of Gold Nanoparticles-Bioconjugated Respiratory Syncytial Virus Infecting HEp-2 Cells. *Sci. Rep.* **2014**, *4*, 4529.
(20) Liu, Y.; Huang, C. Real-Time Dark-Field Scattering Microscopic Monitoring of the In Situ Growth of Single Ag@Au Nanoalloys. *ACS Nano* **2013**, *7*, 11026−11034.
(21) Chen, H.; Shao, L.; Li, Q.; Wang, J. Gold Nanorods and Their Plasmonic Properties. *Chem. Soc. Rev.* **2013**, *42*, 2679−2724.
(22) Liao, H.; Hafner, J. H. Gold Nanorod Bioconjugates. *Chem. Mater.* **2005**, *17*, 4636−4641.
(23) Wang, J.; You, M.; Zhu, G.; Shukoor, M.; Mohammed, I.; Chen, Z.; Zhao, Z.; Altman, M.; Yuan, Q.; Zhu, Z.; Chen, Y.; Huang, C.; Tan, W. Photosensitizer-Gold Nanorod Composite for Targeted Multimodal Therapy. *Small* **2013**, *9*, 3678−3684.
(24) Wang, J.; Zhu, G.; You, M.; Song, E.; Shukoor, M.; Zhang, J.; Altman, M.; Chen, Y.; Zhu, Z.; Huang, C.; Tan, W. Assembly of Aptamer Switch Probes and Photosensitizer on Gold Nanorods for Targeted Photothermal and Photodynamic Cancer Therapy. *ACS Nano* **2012**, *6*, 5070−5077.
(25) Murphy, C. J.; Gole, A. M.; Hunyadi, S. E.; Stone, J. W.; Sisco, P. N.; Alkilany, A.; Kinard, B. E.; Hankins, P. Chemical Sensing and Imaging with Metallic Nanorods. *Chem. Commun.* **2008**, *44*, 544−557.
(26) Becker, J.; Zins, I.; Jakab, A.; Khalavka, Y.; Schubert, O.; Sonnichsen, C. Plasmonic Focusing Reduces Ensemble Linewidth of Silver-Coated Gold Nanorods. *Nano Lett.* **2008**, *8*, 1719−1723.
(27) Zhang, C.; Yin, A.; Jiang, R.; Rong, J.; Dong, L.; Zhao, T.; Sun, L.; Wang, J.; Chen, X.; Yan, C. Time−Temperature Indicator for Perishable Products Based on Kinetically Programmable Ag Overgrowth on Au Nanorods. *ACS Nano* **2013**, *7*, 4561−4568.
(28) Liu, Y.; Schanze, K. S. Conjugated Polyelectrolyte-Based Real-Time Fluorescence Assay for Alkaline Phosphatase with Pyrophosphate as Substrate. *Anal. Chem.* **2008**, *80*, 8605−8612.
(29) Hayat, A.; Andreescu, S. Nanoceria Particles as Catalytic Amplifiers for Alkaline Phosphatase Assays. *Anal. Chem.* **2013**, *85*, 10028−10032.
(30) Lohse, S. E.; Burrows, N. D.; Scarabelli, L.; Liz-Marzan, L. M.; Murphy, C. J. Anisotropic Noble Metal Nanocrystal Growth: the Role of Halides. *Chem. Mater.* **2014**, *26*, 34−43.
(31) Ming, T.; Feng, W.; Tang, Q.; Wang, F.; Sun, L.; Wang, J.; Yan, C. Growth of Tetrahexahedral Gold Nanocrystals with High-Index Facets. *J. Am. Chem. Soc.* **2009**, *131*, 16350−16351.
(32) Gole, A.; Murphy, C. J. Seed-Mediated Synthesis of Gold Nanorods: Role of the Size and Nature of the Seed. *Chem. Mater.* **2004**, *16*, 3633−3640.
(33) Nikoobakht, B.; EI-Sayed, M. A. Preparation and Growth Mechanism of Gold Nanorods (NRs) Using Seed-Mediated Growth Method. *Chem. Mater.* **2003**, *15*, 1957−1962.
(34) Li, Q.; Jiang, R. B.; Ming, T.; Fang, C. H.; Wang, J. F. Crystalline Structure-Dependent Growth of Bimetallic Nanostructures. *Nanoscale* **2012**, *4*, 7070−7077.
(35) Lee, P. C.; Meisel, D. Adsorption and Surface-Enhanced Raman of Dyes on Silver and Gold Sols. *J. Phys. Chem.* **1982**, *86*, 3391−3395.
(36) Xu, L.; Zong, C.; Zheng, X.; Hu, P.; Feng, J.; Ren, B. Label-Free Detection of Native Proteins by Surface-Enhanced Raman Spectroscopy Using Iodide-Modified Nanoparticles. *Anal. Chem.* **2014**, *86*, 2238−2245.
(37) Zhou, C.; Zhao, J.; Pang, D.; Zhang, Z. Enzyme-Induced Metallization as a Signal Amplification Strategy for Highly Sensitive Colorimetric Detection of Avian Influenza Virus Particles. *Anal. Chem.* **2014**, *86*, 2752−2759.
(38) Gao, Z.; Hou, L.; Xu, M.; Tang, D. Enhanced Colorimetric Immunoassay Accompanying with Enzyme Cascade Amplification Strategy for Ultrasensitive Detection of Low-Abundance Protein. *Sci. Rep.* **2014**, *4*, 3966.
(39) Kokado, A.; Arakawa, H.; Maeda, M. New Electrochemical Assay of Alkaline Phosphatase Using Ascorbic Acid 2-Phosphate and Its Application to Enzyme Immunoassay. *Anal. Chim. Acta* **2000**, *407*, 119−125.
(40) Chen, H.; Wang, F.; Li, K.; Woo, K.; Wang, J.; Li, Q.; Su, L.; Zhang, X.; Lin, H.; Yan, C. Plasmonic Percolation: Plasmon-Manifested Dielectric-to-Metal Transition. *ACS Nano* **2012**, *6*, 7162−7171.
(41) Wang, F.; Shen, Y. General Properties of Local Plasmons in Metal Nanostructures. *Phys. Rev. Lett.* **2006**, *97*, 206806.
(42) Martinez, A. W.; Phillips, S. T.; Carrilho, E.; Thomas, S. W., III; Sindi, H.; Whitesides, G. M. Simple Telemedicine for Developing Regions: Camera Phones and Paper-Based Microfluidic Devices for Real-Time, Off-Site Diagnosis. *Anal. Chem.* **2008**, *80*, 3699−3707.
(43) Wang, X.; Meier, R. J.; Link, M.; Wolfbeis, O. S. Photographing Oxygen Distribution. *Angew. Chem., Int. Ed.* **2010**, *49*, 4907−4909.
(44) Vella, S. J.; Beattie, P.; Cademartiri, R.; Laromaine, A.; Martinez, A. W.; Phillips, S. T.; Mirica, K. A.; Whitesides, G. M. Measuring Markers of Liver Function Using a Micropatterned Paper Device Designed for Blood from a Fingerstick. *Anal. Chem.* **2012**, *84*, 2883−2891.